Biomechanical Analysis of Fixation Devices for Lumbar Interbody Fusion

Joana Maria Lemos Ferreira Real
joana.real@tecnico.ulisboa.pt

Instituto Superior Técnico, Lisboa, Portugal

October 2019

Abstract

Disorders of the lumbar spine constitute an important cause of disability. Different approaches to lumbar fusion have been developed throughout the years, in terms of the surgery procedure, the implants and the additional fixation. Although commonly used, fusion still poses some risks, such as the degeneration of the adjacent segment. Finite Element models can be useful tools to increase the understanding of these problems. The objective of this work was the simulation of the biomechanical response of the spine after an Oblique Lumbar Interbody Fusion procedure. This was achieved using an idealized model of the L3 to L5 spine, designed in Solidworks® and implemented in Abaqus®. It comprised the vertebrae, intervertebral discs and ligaments. The intact model, the instrumented one and both of them with disc properties altered to represent degeneration, were then loaded with a follower load of 100 N and a moment of 7.5 Nm to simulate extension, flexion, axial rotation and lateral bending. The range of motion, stress on the adjacent disc and on the instrumentation could then be evaluated. The bilateral model performed better in terms of restricting the range of motion at the fusion segment and achieving lower Von Mises stress on the posterior fixation. However, studies with more complex models are required to assess the ability of the unilateral and cage only models to ensure adequate fusion. No difference was found in the stress on the adjacent disc for the different fixations, but stress increased after the instrumentation was applied, which may lead to degeneration.

Keywords: Lumbar spine, Oblique Lumbar Interbody Fusion, Finite Element model

1. Background

Lumbar spine conditions related with degeneration can greatly impact people's quality of life. They include degenerative disc disease, spondylolisthesis and stenosis, and can cause symptoms such as low back pain [1]. To better treat spinal instability and create implants, understanding the kinematics of the spine is very important. Finite Element (FE) models provide a good tool for that study and allow the comparison between different interventions [2].

One option for the treatment of low back pain is spinal fusion, where a cage is inserted as a replacement of the Intervertebral Disc (IVD), with bone graft in its interior or around it [3]. Different designs have been developed using various materials. In an FE study of the cervical spine [4] it was concluded that the increased Young's Modulus of a titanium cage caused a low relative density in the bone graft when compared with an autograft model or with the PEEK cage. This treatment, however, may present some risks, namely accelerated degeneration of the adjacent level and pseudarthrosis [5].

The access to the spine can be done through the back, by performing a Posterior or Transforaminal Lumbar Interbody Fusion (PLIF or TLIF), anteriorly, in an ALIF, or laterally, through an Extreme or Oblique approach (XLIF and OLIF, respectively). The procedures have different indications and disadvantages. PLIF may include a laminectomy and poses a risk for nerve root injury, while in TLIF the facet joints on one side are removed and there is the danger of paraspinal muscle injury. Lateral procedures, however, preserve the posterior column and don't have the ALIF risk of vascular lesions [6], [7].

These procedures can be supplemented with unilateral or bilateral posterior fixation. On the one hand, bilateral fixation leads to a greater Range Of Motion (ROM) restriction and smaller stresses on the Annulus Fibrosus (AF) and instrumentation, as shown in [8] for TLIF. On the other hand, [9] showed that unilateral fixation caused stability similar to the bilateral one in TLIF, after achieving bone graft fu-

sion. Furthermore, in a meta-analysis of PLIF studies, they showed to be similar in terms of fusion, but the unilateral model provided shorter hospital stay and smaller blood loss and operative time [10]. Despite this, there is no consensus on the best option.

The goal of this work was the simulation of the biomechanical response of the spine in the case of an Oblique Lumbar Interbody Fusion (OLIF) procedure, wherein only the cage is inserted or when it is aided by unilateral or bilateral posterior fixation. Degeneration was also simulated to understand its effect on the spine. To achieve this, an idealized CAD model of two vertebral segments was developed and validated.

The present work may be useful to the surgical practice in understanding the pros and cons of the different types of fixation and the impact they have on the adjacent segment since it can degenerate as a consequence of the altered stress distribution after fusion [12].

2. Methodology

2.1. Intact Model

Each vertebra was built in Solidworks® (Dassault Systèmes SolidWorks Corp., USA), using a vertebral body, with cortical and trabecular bone, of a past work [11], and adding the posterior elements, as shown in Figure 1. After the model of the vertebra was completed, an assembly was created. The vertebrae were set to make an angle of 7 degrees with each other and an IVD with a height of around 10 mm was created between each pair, with the Nucleus Pulposus (NP) distinguished from the AF.

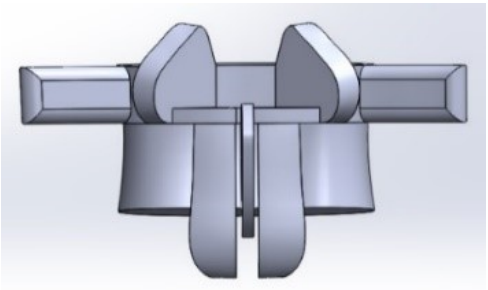

Figure 1: Posterior view of the model of one lumbar vertebra.

The model was imported to Abaqus® (Dassault Systèmes Simulia Corp., USA) and the materials were assigned to each section, with the parameters shown in Table 1. An assembly was formed, and the geometry was merged, retaining the intersecting boundaries. The fibers of the AF were set to make an angle of 35° or 145° with the normal in consecutive layers, as seen in [13]. The ligaments were then added to the model: Ligamentum Flavum (LF), Intertransverse Ligaments (ITL), Interspinous Ligaments (ISL), Supraspinous Ligaments (SSL), Capsular Ligaments (CL), Anterior Longitudinal Ligament (ALL), and Posterior Longitudinal Ligaments (PLL). The choice of the attachment points and the number of ligaments of each type was done based on [13], [14]. They were created as parts of the type wire with length equal to the distance between a pair of points and constrained to be parallel to an axis passing through them. Couplings of the type continuum distributing were created at every ligament insertion point, so that it was attached to the surface of the vertebrae, considering an influence radius of 2.

2.2. Selection of Ligament Properties

The ROM obtained for the model under moments of 10, 7.5, 5, 2.5 and 1 Nm simulating Extension (E), Flexion (Flex), Axial Rotation (AR) and Lateral Bending (LB) was compared to the results obtained by Heuer et al. [15] for cadaver L4-L5 segments without ITL. This allowed the choice of the Young's modulus [16] and the cross-sectional area [17] of the ligaments from the wide range present in the literature. The final set of values, in Table 2, allowed around 75 % of the simulations to be within the range in [15]. The ligaments could then be assigned a section of the type truss with those properties.

2.3. Instrumented Model

The cage for the OLIF procedure, the screws and the bars that connect the latter were designed in Solidworks® following the guidelines of the Medtronic guide [18]. The cage had a length of 40 mm, width of 22 mm and height of 12 mm and was made of PEEK (E = 3600 MPa; ν = 0.38, [19]). The screws and bars had a diameter of 5.5 mm and a length of 45 mm and were made of Titanium (E = 105000 MPa; ν = 0.34, [20]).

Table 1: Constitutive models and parameters used in Abaqus®. All values were taken from [11].

Material	Formulation	Parameters	
Cortical Bone	Linear Elastic	E (MPa)	12000
		ν	0.3
Trabecular Bone	Linear Elastic	E (MPa)	200
		ν	0.315
Annulus Fibrosus	Hyperelastic Anisotropic (Holzapfel)	C10	0.315
		D1	0.254
		k1 (MPa)	12
		K2	300
		kappa	0.1
Nucleus Pulposus	Hyperelastic Isotropic (Mooney-Rivlin)	C10	0.12
		C01	0.03
		D1	0.6667

Table 2: Ligament properties after validation.

Ligament	Young Modulus (MPa)	Cross-sectional Area of each ligament (mm^2)
ALL	17.0	14.0
PLL	20.0	6.7
CL	33.0	11.7
LF	19.5	38.0
ISL	10.0	10.0
SSL	10.0	14.0
ITL	58.7	5.0

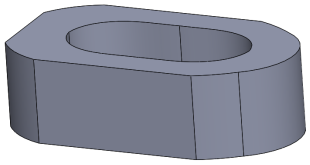

Figure 2: OLIF cage

The IVD between L4 and L5 was removed and replaced with the cage, thus forming the instrumented model without posterior fixation (cage only). From that one, three other models were created: one with screws inserted through the left pedicles of L4 and L5 and a bar connecting them (unilateral left), one with the screws inserted through the right pedicles (unilateral right) and one with bilateral posterior fixation (bilateral), as seen in Figure 3.

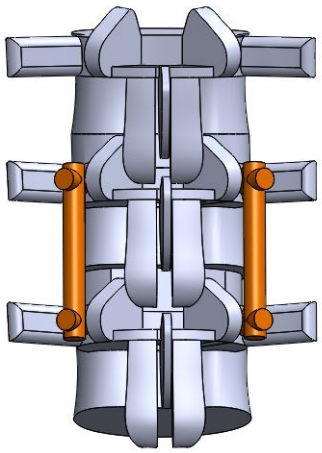

Figure 3: L3-L5 model with bilateral posteiror fixation.

2.4. Convergence Study

A vertical downward displacement equal to 1 mm, around 10% of the IVD height, was applied on a reference point coupled to the superior surface. It was then possible to generate meshes of different sizes and evaluate the Von Mises stress on a node on the interface between L3 and the upper IVD. The chosen mesh element size, 2 mm, was the one for which the stress did not depend on the number of elements anymore. Partitions were created on some surfaces to choose the ligament attachment points more easily and the element growth rate was increased. The final number of elements of type C3D4 was 131760 and, after the ligaments were meshed as linear trusses, with an element size that produced only one element per ligament, 172 elements of type T3D2 were added to the mesh, which had a total of 27246 nodes.

2.5. Boundary conditions

The value of the Follower Load (FL) was chosen by performing simulations under the same moments as for the selection of ligament properties, plus different preloads. The preload of 100 N was the one that produced better results compared to [15]. Two steps were created, the first for the implementation of an FL of 100 N, causing compression and following nodal rotation and the second with the propagated FL and a moment of 7.5 Nm to simulate the different motions. Both loads were applied in a referential with origin at the center of the upper surface of L3. The point was coupled to the surface so that the loads were equally distributed by all the nodes.

To restrain the movement of the model, the bottom surface (the base of the L5 vertebral body) was fixed with an *Encastre* boundary condition. To prevent each pair of articular processes from intersecting, a surface to surface contact constraint with exponential pressure overclosure was created, as seen in [2]. The parameters were changed until they completely prevented intersection and finally were set to a pressure of 50 N/mm^2 and a clearance of 1 mm. Additionally, to prevent the inferior articular processes from intersecting the laminae below, a surface to surface contact constraints for tangential behavior with a penalty of 0.5 were created.

All the constitutive parts, except the cage, were merged to simulate complete osteointegration of the screws and to prevent movement of the screws relative to the bar. The cage-bone interface was modeled with a *Tie* constraint to simulate the long-term integration situation. In the case of the instrumented models, the only constraints performed to prevent intersection were the ones between the inferior articular processes of L3 and the superior articular processes of L4.

The total ROM was obtained by considering a vector uniting two points of the upper L3 vertebra (on the anterior and posterior extremes for E, Flex and AR, and on the lateral extremes for LB) and calculating the angle the vector before motion

made with the vector after motion. In the case of the segmental ROM, the one for the L4-L5 level was obtained by measuring the angular motion of the L4 vertebra relative to the constricted L5 one, as described above for the whole model. Then, the L3-L4 segmental ROM was calculated by subtracting the L4-L5 angle from the total ROM, thus achieving the angular motion of the L3 vertebra relative to the one below.

2.6. Simulation of Degeneration

Ruberté et al. [21] simulated two stages of degeneration of the IVD of the L4-L5 level by reducing the disc height and the area of the NP, increasing the laxity of the ALL, PLL and the fibers of the AF, and changing the properties of the AF and NP. In the present study, however, degeneration was simulated only by the latter. The properties given in [21] had to be converted to the parameters of the Mooney-Rivlin formulation used in this model.

Cavalcanti et al. [22] developed a model of the AF, wherein they distinguished four different regions. Since the AF fibers lose part of their ability to withstand pressure, they were modeled as being laxer in the mildly degenerated case than in the healthy, and further still in the moderately degenerated. Hence the fibers in mild degeneration had the same parameters as the ventral internal region in [22] and in moderate degeneration they had the same values as the dorsal internal. The final parameters used to simulate degeneration can be seen in Table 3.

3. Results

3.1. Degenerated models

To understand the implications of degeneration on the biomechanics of the spine, simulations were made with each disc either healthy, mildly or moderately degenerated, resulting in the following cases: 1) both discs healthy; 2) L3-L4 healthy and L4-L5 mild; 3) both discs mild; 4) L3-L4 healthy and L4-L5 moderate; 5) L3-L4 mild and L4-L5 moderate.

As shown in Table 4, for E, Flex and LB the spine suffered a ROM decrease as degeneration progressed, while in AR the ROM increased when compared to the intact model but did not follow a trend.

3.2. Instrumented models

Instrumentation produced a reduction of the total ROM compared to the non-instrumented model for all motions. For the L3-L4 segment, as can be seen in Table 5, in E and Flex, the segmental ROM increased relative to the healthy case for all constructs, but that gain decreased from no posterior fixation to bilateral. For left AR, all the percentage changes were very small. In right LB, the ROM was greater than in the healthy case for all constructs, however, the unilateral left model was the one that caused the smallest increase.

The instrumentation caused a considerable decrease in the segmental ROM of the L4-L5 spinal unit, as per Table 6. For all the motions this restriction of movement was bigger in the unilateral model than in the cage only one, and even greater for the bilateral model. The movement that was more successfully constrained was LB, with a change of approximately 96% for the bilateral model. The various types of fixation caused similar results in AR and LB, while the result for Flex appeared to depend more on the instrumentation. Extension granted the highest disparity among models, with the cage only case decreasing the ROM in around 80% and the bilateral model managing to reduce it by 91%.

3.3. Degenerated instrumented models

In the L3-L4 segment, as seen in Table 7, AR presented a considerable change, with values 62-63% greater in the degenerated case. Flex and LB pre-

Table 3: Coefficients used in the present work's material formulations of the AF and NP for the healthy, mildly degenerated and moderately degenerated cases.

Degree of degeneration	Annulus Fibrosus				Nucleus Pulposus		
	C10	D1	K1 (Mpa)	K2	C10	C01	D1
Healthy	0.315	0.254	12	300	0.12	0.03	0.667
Mild	0.5	0.32	1.74	43.5	0.168	0.042	0.476
Moderate	1.13	0.14	0.435	8.7	0.221	0.055	0.723

Table 4: ROM, in degrees, obtained for the four movements for different combinations of degeneration states of the discs.

Movement	Case (1) (deg)	Case (2) (deg)	Case (3) (deg)	Case (4) (deg)	Case (5) (deg)
E	3.84	3.82	3.79	3.58	3.56
Flex	5.85	5.56	5.24	4.89	4.57
Left AR	4.36	5.47	6.80	4.97	6.31
Right LB	6.72	6.63	6.49	5.69	5.56

Table 5: ROM of the L3-L4 segment, in degrees, for the healthy and instrumented cases.

Movement	Healthy (deg)	Cage only (deg)	Unilat. Left (deg)	Unilat. Right (deg)	Bilateral (deg)
E	2.08	2.21	2.16	2.18	2.15
Flex	2.99	3.32	3.31	3.30	3.29
Left AR	2.26	2.24	2.23	2.23	2.23
Right LB	3.66	3.82	3.77	3.81	3.79
Right AR	—	—	2.16	2.16	—
Left LB	—	—	3.82	3.79	—

Table 6: ROM of the L4-L5 segment, in degrees, for the healthy and instrumented cases.

Movement	Healthy (deg)	Cage only (deg)	Unilat. Left (deg)	Unilat. Right (deg)	Bilateral (deg)
E	1.75	0.36	0.22	0.22	0.16
Flex	2.86	0.36	0.26	0.26	0.20
AR left	2.10	0.24	0.22	0.21	0.20
LB right	3.06	0.16	0.14	0.15	0.12
Right AR	—	—	0.21	0.22	—
Left LB	—	—	0.14	0.14	—

sented a decreased ROM compared to the healthy instrumented model, although the change was less appreciable than that of AR. In E, the ROM increased for the cage only model and decreased for the other three constructs.

The changes in the segmental L4-L5 ROM, were not significant compared to the values obtained for the same instrumentation with the adjacent disc healthy, except for E in the cage only model.

3.4. Equivalent Pressure Stress

Considering just the NP of the upper level, the maximum pressure for the non-instrumented, instrumented with adjacent disc healthy and instrumented with adjacent disc mildly degenerated models were compared, as presented in Table 8. The instrumented model showed pressure values around 17% higher than the non-instrumented case, in all movements except LB. When analyzing the degenerated disc, except AR which had a 31% pressure decrease, the NP was subjected to higher pressure, with E presenting the highest percentage change (around 48%).

3.5. Von Mises Stess on the Posterior Fixation

Considering the comparison of the two unilateral models in AR and LB is done when both are rotating/bending to the same side or to the opposite side of instrumentation, the unilateral right showed smaller maximum Von Mises stress in all movements except Flex, as can be seen in Table 9. The difference between the two was more substantial when bending to the opposite side of fixation and in E. The bilateral model showed smaller maximum Von Mises stress on the screws and rod of each side than the unilateral model of the correspondent side. Once again, the biggest differences were seen for Flex.

4. Discussion

With increasing degeneration, the only movement for which the spine became more mobile than in the healthy state was AR. The increase in AR was also seen in the literature for cadaver spinal units [23].

A study simulating TLIF in an L1-S1 spine [8] found that, at the level of the intervention, the ROM was smaller in the bilateral case (when compared to the values of the unilateral, 15 to 22% in E, 26 to 32% in right AR and 27 to 59% in right LB). In the present study also, bilateral posterior fixation achieved smaller L4-L5 ROM in all movements, with a similar ROM percentage change in E (27 to 29%, relative to the values of the unilateral fixation). However, it had also a significant decrease in Flex (22%), a non-significant decrease for AR and a less intense reduction for LB (15 to 19%).

In another study [24], the authors created an L3-L5 model and found no ROM differences for the adjacent segment compared to the intact model, as happened in the present study (the highest percentage change was 11% for the cage only model in Flex).

In [25] for all movements, the authors found an increase in the pressure the NP was subjected to after PLIF, compared to the intact case. This increase was especially noticeable in E (around 33%). With degeneration the pressure further increased, particularly for AR and E. In the present work, E, Flex and AR had a similar maximum pressure increase (around 17%), while there was no variation for LB. With degeneration, LB showed the smallest change, whereas E and Flex had a considerable increase, greater than in the literature. With the exception of AR, the results show that the NP is put under more pressure after the intervention and further still with degeneration of the adja-

Table 7: ROM of the L3-L4 segment, in degrees, of the instrumented models with the adjacent disc mildly degenerated.

Movement	Cage only (deg)	Unilat. Left (deg)	Unilat. Right (deg)	Bilateral (deg)
E	2.43	2.14	2.16	2.14
Flex	2.97	2.97	2.96	2.95
Left AR	3.64	3.63	3.63	3.62
Right LB	3.68	3.64	3.67	3.65
Right AR	—	3.56	3.55	—
Left LB	—	3.65	3.62	—

cent segment.

Ambati et al. [24] developed an L3-L5 model, simulated fusion at the bottom segment and measured the stress on the posterior instrumentation. They found that the stress on the left unilateral screws was higher than that of the bilateral (2.7 to 6.3 times in flexion, 1.2 to 1.7 times in extension, 2 to 4.1 times in left LB and 1.4 to 2.4 in right LB, while there were no big differences in AR). Although in the present study the unilateral fixation showed higher maximum Von Mises stress as well (except for the unilateral left in left LB and the unilateral right in right AR), the differences between the two types of fixation were not as marked as in the literature. It is worth mentioning that in [24] the procedure simulated was TLIF and thus all the cages were different from the one used in the present study, and so impact the posterior fixation differently.

Lastly, all the maximum Von Mises stresses on the posterior fixation devices were really small compared to the ultimate tensile stress of the titanium alloy considered (around 900 MPa, [20]), so the values found in the instrumentation don't pose a risk of failure.

5. Conclusion and Future work

The results of the present study can be summarized as follows:

i) With the progression of degeneration, the spine became more unstable for AR.

ii) Bilateral posterior fixation caused a greater reduction in ROM than the unilateral one, which in turn reduced the ROM more than the cage only model. Following the reasoning that a near-immobile segment is preferred for achieving adequate fusion, the bilateral posterior fixation should be the most satisfactory one.

iii) The pressure on the adjacent NP increased from healthy to instrumented and further to the degenerated instrumented models.

iv) The instrumentation was subjected to a higher Von Mises stress in the unilateral fixation case, though the stress values were under the ultimate tensile stress for titanium.

The model in the present work was limited since it was idealized and not based on medical images. It comprised only two motion segments, which does not give the panorama of the whole lumbar spine. In the simulation of degeneration only the parameters of the formulations were altered, while the height was kept constant. Finally, the lordotic angle and the teeth of the cage were neglected, and the cage-vertebra interaction was considered to be a *Tie* constraint, which only accounts for the stage after fusion.

In the future, the same tests should be performed on a more complex model, which might be

Table 8: Maximum Pressure acting on the NP, in MPa, for the non-instrumented model and the model instrumented with bilateral fixation and an adjacent disc healthy or mildly degenerated.

Movement	Healthy (MPa)	Instrumented (MPa)	Degenerated instrumented (MPa)
E	0.079	0.092	0.118
Flex	0.224	0.261	0.287
Left AR	0.202	0.238	0.140
Right LB	0.321	0.322	0.369

Table 9: Maximum Von Mises stress, in MPa, on the posterior instrumentation for all types of constructs.

Movement	Unilat. Left	Unilat. Right	Bilateral	
			Left	Right
E	41.79	35.62	40.03	28.26
Flex	38.75	42.45	28.17	32.13
Left AR	28.78	33.57	24.59	31.06
Right LB	38.84	22.7	32.34	18.08
Right AR	34.64	26.51	—	—
Left LB	23.48	29.99	—	—

altered to replicate specific diseases or conditions. Furthermore, it is necessary to understand the effects of instrumentation on the adjacent disc since in the present work it was more loaded than the intact, which may lead to degeneration.

Aknowledgement: *This document was written and made publicly available as an institutional academic requirement and as a part of the evaluation of the MSc thesis in Biomedical Engineering of the author at Instituto Superior Técnico. The work described herein was performed at the Department of Mechanical Engineering of Instituto Superior Técnico (Lisbon, Portugal), during the period February-October 2019, under the supervision of Prof. Paulo Fernandes and Prof. André Castro.*

References

[1] V. M. Ravindra et al., "Degenerative Lumbar Spine Disease: Estimating Global Incidence and Worldwide Volume," Glob. Spine J., vol. 8, pp. 784–794, 2018.

[2] B. Weisse, A. K. Aiyangar, C. Affolter, R. Gander, G. P. Terrasi, and H. Ploeg, "Determination of the translational and rotational stiffnesses of an L4-L5 functional spinal unit using a specimen-specific finite element model," J. Mech. Behav. Biomed. Mater., vol. 13, pp. 45–61, 2012.

[3] T. Steffen, A. Tsantrizos, I. Fruth, and M. Aebi, "Cages: designs and concepts," Eur. Spine J., vol. 9, pp. 89–94, 2000.

[4] L. C. Espinha, P. R. Fernandes, and J. Folgado, "Computational analysis of bone remodeling during an anterior cervical fusion," J. Biomech., vol. 43, pp. 2875–2880, 2010.

[5] A. H. Khalifa, T. Stübig, O. Meier, and C. W. Müller, "Dynamic stabilization for degenerative diseases in the lumbar spine: 2 years results," Orthop. Rev., vol. 10, pp. 26–31, 2018.

[6] C. Schizas, G. Kulik, and V. Kosmopoulos, "Disc degeneration: current surgical options," Eur. Cells Mater., vol. 20, pp. 306–315, 2010.

[7] R. J. Mobbs, K. Phan, G. Malham, K. Seex, and P. J. Rao, "Lumbar interbody fusion: techniques, indications and comparison of interbody fusion options including PLIF, TLIF, MI-TLIF, OLIF/ATP, LLIF and ALIF," J. spine Surg., vol. 1, pp. 2–18, 2015.

[8] S. H. Chen, S. C. Lin, W. C. Tsai, C. W. Wang, and S. H. Chao, "Biomechanical comparison of unilateral and bilateral pedicle screws fixation for transforaminal lumbar interbody fusion after decompressive surgery - A finite element analysis," BMC Musculoskelet. Disord., vol. 13, 2012.

[9] J. Li, W. Wang, R. Zuo, and Y. Zhou, "Biomechanical Stability Before and After Graft Fusion with Unilateral and Bilateral Pedicle Screw Fixation: Finite Element Study," World Neurosurg., vol. 123, pp. 228–234, 2019.

[10] K. S. Suk, H. M. Lee, N. H. Kim, and J. W. Ha, "Unilateral versus bilateral pedicle screw fixation in lumbar spinal fusion," Spine., vol. 25, pp. 1843–1847, 2000.

[11] R. Guerreiro, "Biomechanical effects of different lumbar fusion cage designs," 2018.

[12] C. S. Chen, C. K. Cheng, C. L. Liu, and W. H. Lo, "Stress analysis of the disc adjacent to interbody fusion in lumbar spine," Med. Eng. Phys., vol. 23, pp. 485–493, 2001.

[13] S. Naserkhaki, J. L. Jaremko, and M. El-Rich, "Effects of inter-individual lumbar spine geometry variation on load-sharing: Geometrically personalized Finite Element study," J. Biomech., vol. 49, pp. 2909–2917, 2016.

[14] S. Naserkhaki, N. Arjmand, A. Shirazi-Adl, F. Farahmand, and M. El-Rich, "Effects of eight different ligament property datasets on biomechanics of a lumbar L4-L5 finite element model," J. Biomech., vol. 70, pp. 33–42, 2018.

[15] F. Heuer, H. Schmidt, Z. Klezl, L. Claes, and H. Wilke, "Stepwise reduction of functional spinal structures increase range of motion and change lordosis angle," J. Biomech., vol. 40, pp. 271–280, 2007.

[16] A. M. Ellingson, M. N. Shaw, H. Giambini, and K. N. An, "Comparative role of disc degeneration and ligament failure on functional mechanics of the lumbar spine," Comput. Methods Biomech. Biomed. Engin., vol. 19, pp. 1009–1018, 2015.

[17] R. Eberlein, G. A. Holzapfel, and M. Fröhlich, "Multi-segment FEA of the human lumbar spine including the heterogeneity of the annulus fibrosus," Comput. Mech., vol. 34, pp. 147–163, 2004.

[18] Medtronic, "Oblique Lateral Interbody Fusion For L2 to L5 Surgical Technique."

[19] J. Cegoñino, A. Calvo-Echenique, and A. Pérez-Del Palomar, “Influence of different fusion techniques in lumbar spine over the adjacent segments: A 3D finite element study,” J. Orthop. Res., vol. 33, pp. 993–1000, 2015.

[20] L. Klein, “TITAN Grade Nb TiAl6Nb7.”

[21] L. M. Ruberté, R. N. Natarajan, and G. B. Andersson, “Influence of single-level lumbar degenerative disc disease on the behavior of the adjacent segments-A finite element model study,” J. Biomech., vol. 42, pp. 341–348, 2009.

[22] C. Cavalcanti, H. Correia, A. Castro, and J. L. Alves, “Constituive modelling of the annulus fibrosus: Numerical implementation and numerical analysis,” 3rd Port. Bioeng. Meet. ENBENG 2013 - B. Proc., vol. 7, pp. 3–6, 2013.

[23] M. Krismer, C. Haid, H. Behensky, P. Kapfinger, F. Landauer, and F. Rachbauer, “Motion in Lumbar Functional Spine Units During Side Bending and Axial Rotation Moments Depending on the Degree of Degeneration,” Spine., vol. 25, pp. 2020–2027, 2000.

[24] D. V Ambati, E. K. Wright, R. A. Lehman, D. G. Kang, S. C. Wagner, and A. E. Dmitriev, “Bilateral pedicle screw fixation provides superior biomechanical stability in transforaminal lumbar interbody fusion: a finite element study,” The Spine Journal., 2014.

[25] S. Jiang and W. Li, “Biomechanical study of proximal adjacent segment degeneration after posterior lumbar interbody fusion and fixation: A finite element analysis,” J. Orthop. Surg. Res., vol. 14, 2019.